disease induction in a similar hierarchy. Finally, a mixture of the immunodominant determinants of MBP (Ac 1–11 and 35–47) delivered in a tolerogenic manner successfully treated ongoing disease by inducing anergy in the antigen-specific T cells.

REFERENCES AND NOTES

1. A. Oki and E. Sercarz, *J. Exp. Med.* **161**, 897 (1985).
2. G. Gammon *et al.*, *Nature* **319**, 413 (1986).
3. F. Ria, B. M. C. Chan, M. T. Scherer, J. A. Smith, M. L. Gefter, *ibid.* **343**, 381 (1990).
4. J. P. Clayton *et al.*, *J. Exp. Med.* **169**, 1681 (1989).
5. H. M. Wisniewski and A. B. Keith, *Ann. Neurol.* **1**, 144 (1977).
6. We confirmed antigen specificity of the unresponsiveness by treating mice intraperitoneally with a control peptide [amino acids 110 to 121 of sperm whale myoglobin (SWM)] and later immunizing with MBP peptide. Responses to 25 μM Ac 1–11 were similar in both the IFA-treated and SWM (110–121)–treated mice. The radioactivities were 13,576 ± 2,455 cpm (mean ± SEM; $n = 3$) and 14,502 ± 979 cpm for the two groups, respectively. Similarly, MBP peptides given in a tolerogenic manner did not affect the response after immunization of (PL/J × SJL)F_1 mice with 100 μg of an immunogenic peptide [amino acids 39 to 61 from the variable region of the β ($V_β$8.2) chain of the T cell receptor]; the results were 74,193 ± 4,179 cpm for the IFA-treated group and 72,787 ± 7,506 cpm for the MBP peptide–treated group in response to challenge with 5 μM 39–61 TCR peptide.
7. D. E. Smilek *et al.*, *Proc. Natl. Acad. Sci. U.S.A.* **88**, 9633 (1991).
8. R. B. Fritz, C. H. Jen-Chou, D. E. McFarlin, *J. Immunol.* **130**, 191 (1983); S. S. Zamvil *et al.*, *Nature* **324**, 258 (1986).
9. D. H. Kono *et al.*, *J. Exp. Med.* **168**, 213 (1988).
10. S. W. Brostoff and D. W. Mason, *J Immunol.* **133**, 1938 (1984).
11. M. K. Waldor *et al.*, *Science* **227**, 415 (1985).
12. S. S. Zamvil *et al.*, *J. Exp. Med.* **168**, 1181 (1988).
13. S. S. Zamvil *et al.*, *ibid.* **167**, 1586 (1988).
14. H. Acha-Orbea *et al.*, *Cell* **54**, 263 (1988).
15. J. L. Urban *et al.*, *ibid.*, p. 577.
16. D. M. Zaller, G. Osman, O. Kanagawa, L. Hood, *J. Exp. Med.* **171**, 1943 (1990).
17. A. A. Vandenbark, G. Hashim, H. Offner, *Nature* **341**, 541 (1989).
18. M. D. Howell *et al.*, *Science* **246**, 668 (1989).
19. D. A. Hafler *et al.*, *J. Exp. Med.* **167**, 1313 (1988).
20. R. Martin *et al.*, *ibid.* **173**, 19 (1991).
21. R. Martin *et al.*, *J. Immunol.* **148**, 1359 (1992).
22. E. C. Alvord, Jr., C. Shaw, S. Hruby, M. W. Kies, *Ann. N.Y. Acad. Sci.* **1220**, 333 (1965); B. Campbell, P. J. Vogel, E. Fisher, R. Lorenz, *Arch. Neurol.* **29**, 10 (1973); B. F. Driscoll, M. W. Kies, E. C. Alvord, Jr., *J. Immunol.* **117**, 110 (1976); G A. Hashim and F. J. Schilling, *Arch. Biochem. Biophys.* **156**, 287 (1973); E H. Eylan *et al.*, *Nature* **236**, 74 (1972); B. F. Driscoll, M. W. Kies, E. C. Alvord, Jr., *J. Immunol.* **112**, 392 (1974).
23. D. C. Wraith, D. E. Smilek, D. J. Mitchell, L. Steinman, H. O. McDevitt, *Cell* **59**, 247 (1989).
24. T. DeMagistris *et al.*, *ibid.* **68**, 625 (1992).

25. We thank H. Y. Tse for providing guinea pig MBP, L. Steinman and H. O. McDevitt for critical review of the manuscript, and R. Kizer and K. Sturgis for preparation of the manuscript Supported by the Multiple Sclerosis Society and NIH grant AI 27989. A.G. was a fellow of the American Diabetes Association.

18 June 1992; accepted 9 September 1992

Intrinsic Quantal Variability Due to Stochastic Properties of Receptor-Transmitter Interactions

Donald S. Faber,* William S. Young,† Pascal Legendre, Henri Korn

Synaptic events at the neuromuscular junction are integer multiples of a quantum, the postsynaptic response to transmitter released from one presynaptic vesicle. At central synapses where quanta are small, it has been suggested they are invariant due to occupation of all postsynaptic receptors, a concept neglecting inherent fluctuations in channel behavior. If this did occur, the quantal release model would not apply there and could not be used to localize sites of synaptic modification. Monte Carlo simulations of quanta include transmitter diffusion and interactions with postsynaptic receptors that are treated probabilistically. These models suggest that when there are few postsynaptic channels available at a synapse, their stochastic behavior produces significant intrinsic variance in response amplitude and kinetics, and saturation does not occur. These results were confirmed by analysis of inhibitory quanta in embryonic and adult Mauthner cells involving a small and large number of channels, respectively. The findings apply to excitatory synapses as well.

Stochastic properties of ionic channels have not been incorporated in schemes of central synaptic transduction. Rather, it has been assumed that the size and shape of neuronal responses can be accounted for by laws of mass (average) action. Responses are generally modeled by a series of coupled differential equations (*1*, *2*) that do not take intrinsic variations into account. Such computations seem to reinforce the conclusion that quantal events in the central nervous system involving few channels exhibit minimal variance (*3*), particularly when a synaptic vesicle contains a large number of transmitter molecules (*4*). Apparently, quantal size is "saturated" (i) even if not all channels are opened at the response peak (*3*, *5*) or (ii) because the transmitter released always opens all channels (100% saturation) (*6*, but see *7*). If so, quantization of synaptic amplitudes in the central nervous system would not reflect the release process, such as at the neuromuscular junction, but would be a postsynaptic phenomenon (*5*). Also, neurotransmission would be different at peripheral and central junctions.

The quantal parameters used in statistical analyses of synaptic transmission and its modifications would have new meanings. The variables n, the number of available release units or active zones, and P, the probability of release of a quantal packet (*7*, *8*), would be compounded by the number of receptor clusters at a synapse and the likelihood that they are functional. Furthermore, if quantal size, q, were fixed, the 10 to 50% coefficient of variation (CV) of spontaneous events observed in some studies (*9–11*) would arise from activation of different receptor aggregates. Resolution of this issue, which requires characterization of quanta generated at one site, is important for further investigations of the cellular basis of processes underlying synaptic plasticity, such as long-term potentiation. Although quantal analysis may reveal which parameter is modified (*12–14*), a clear model is important because interpretations differ according to the initial assumptions (*7*, *15*).

We have combined experiments in situ with Monte Carlo simulations of quantal events to identify sources of fluctuations at single synapses. The model keeps track of the state of each molecule and computes transitions individually. Its validity was confirmed by electrophysiological verification of testable predictions.

In our model of a central synapse there is one presynaptic release site, a 20-nm cleft, and an apposed postsynaptic membrane with a circular receptor aggregate surrounded by a receptor-free zone (*1*), with a combined diameter of ≥1 μm (*16*). The cleft is subdivided into four layers of more than 100,000 rectangular solids (Fig. 1A). This division defines the volume in Cartesian coordinates (x,y,z), with the center of the release site as the origin. A fifth layer represents the postsynaptic membrane. At time zero, a quantal packet of T transmitter molecules (A) is released, and each is followed in space and time with steps (Δt) of 1 μs. Each molecule's diffusion path (Fig. 1B) is calculated by random selection of an incremental distance and direction along each axis from a distribution function relating the average distance moved to the

D. S. Faber and W. S. Young, Neurobiology Laboratory, State University of New York, Buffalo, NY 14214. P. Legendre and H. Korn, Department of Biotechnologies, Institute Pasteur, INSERM U-261, Paris, France.

*To whom correspondence should be addressed at Department of Anatomy and Neurobiology, Medical College of Pennsylvania, 3200 Henry Avenue, Philadelphia, PA 19129.

†Present address: Mellon Institute, Pittsburgh, PA 15213.

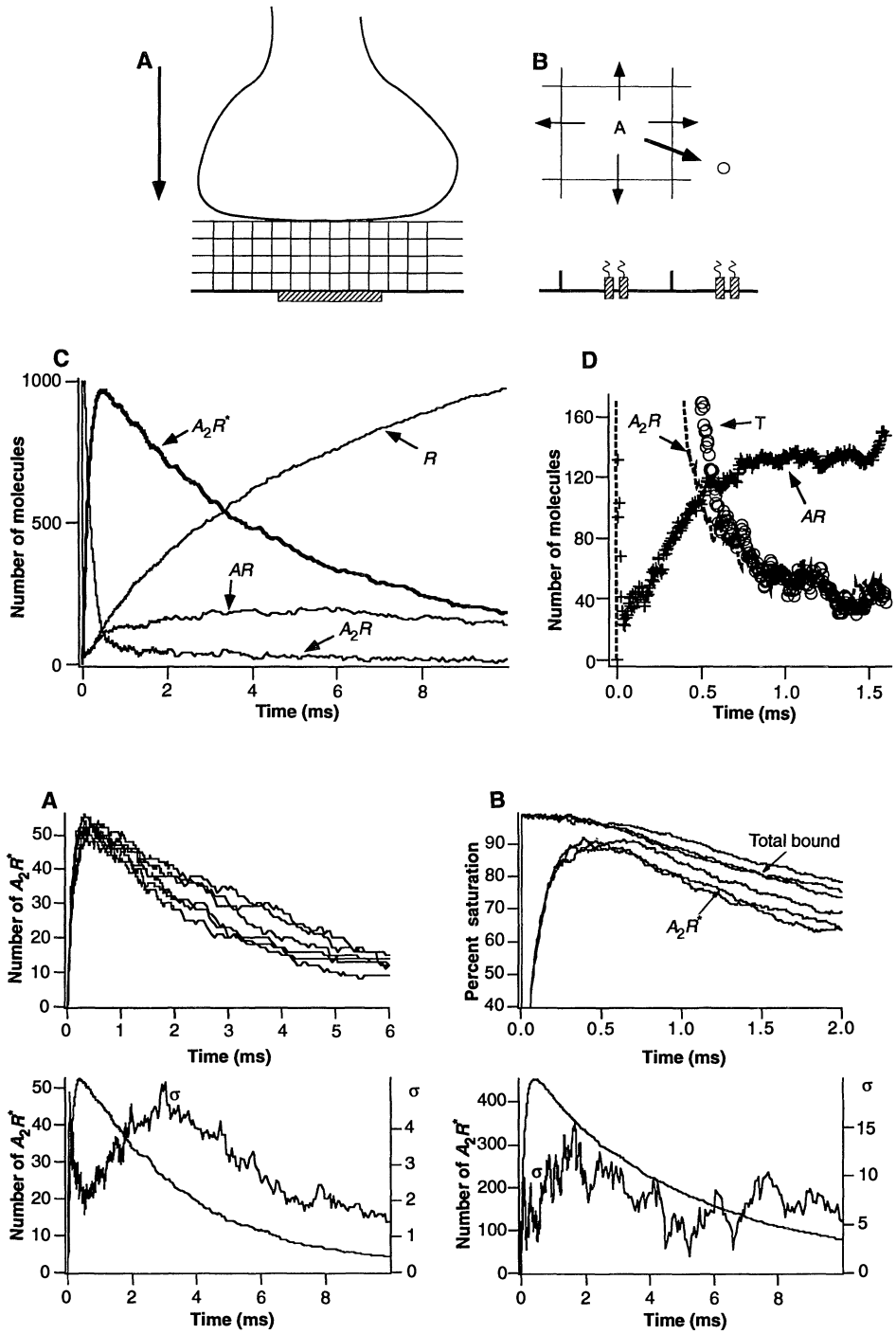

Fig. 1. Fate of transmitter and receptor molecules in a Monte Carlo simulation of a quantal response. (**A**) Transverse representation of a central synapse indicating the presynaptic terminal, the 20-nm synaptic cleft that was divided in the model into four layers of rectangular solids (6 by 6 by 5 nm), and the postsynaptic membrane (thick line) with its receptor area (hatched). (**B**) Expanded view of one "cell" containing an agonist molecule (A) free to move in the horizontal and vertical directions, and a typical destination (circle) reached in Δt. Interactions with receptors (two binding sites) are updated after each time step. (**C**) Time course of the quantal glycinergic response (A_2R^*, double-bound open channels), of single-bound (AR), double-bound closed (A_2R), and free (R) receptors, after release of 10,000 transmitter molecules at $t = 0$, onto a receptor cluster of 1313 channels. The plotted time step is 5 μs for the first 2 ms and 50 μs thereafter. (**D**) Higher gain plot of initial events after the same exocytosis, showing the number of transmitter molecules (T) in the synaptic cleft and the number of receptors in the two bound closed states (AR and A_2R).

diffusion constant D and Δt (*17*). Ligand binding and channel opening or closing depend on the transmitter concentration near the postsynaptic membrane and the state of the receptors (R). The scheme used is

$$2A + R \underset{k_{-1}}{\overset{k_{+1}}{\rightleftharpoons}} AR + A \underset{k_{-2}}{\overset{k_{+2}}{\rightleftharpoons}} A_2R \underset{\alpha}{\overset{\beta}{\rightleftharpoons}} A_2R^*$$

on the assumption of two binding sites per channel (*18*). The rate constants (k_i, α, and β) determine the transition probabilities between states (*19*).

This general algorithm requires optimization of parameters to match simulated responses with those obtained in vivo. Previously determined constraints for the glycinergic quanta of adult M cells were 500 to 1000 activated channels (*8*, *20*) and 0.3 to 0.5 and 4.5 to 7.5 ms for the peak and 1/*e* decay times, respectively (*20*, *21*). With the affinity constant in the micromolar range (*22*), representative values were k_{+1}, $k_{+2} = 4 \times 10^8$ (M^{-1} s^{-1}), which is in the limits allowable by diffusion, $k_{-1} = 1600$ s^{-1} and $k_{-2} = 16{,}000$ s^{-1} (*23*), a β/α ratio = 10 to 20 (typically $\beta = 5000$, $\alpha = 500$), and $D = 0.5$ to 1×10^{-6} cm^2 s^{-1}. Binding site density σ was 15,000/μm^2 (tested range, 3,750 to 30,000), with a receptor matrix 0.46 μm in diameter (*1*, *24*). Quantal size (the number of opened channels) can be varied by a change in one or both of the last two parameters. We kept σ constant to provide conditions most favorable for saturation. Thus, data reported for small quanta correspond to restricted receptor clusters.

A typical simulated quantum with 970 opened channels is illustrated in Fig. 1C, along with the time courses of change in the numbers of receptors in the different closed states. The persistent elevation of single-bound complexes, shown with better resolution in Fig. 1D (because k_{-1} is ten times slower than k_{-2}), provides the substrate for facilitative interactions between adjacent synapses (*24*). With the fast diffusion constant used, the amount of free transmitter in the cleft falls to 1% of its initial value by the response peak (Fig. 1B), indicating that variations in the decay phase are not produced by residual transmitter.

Fig. 2. Fluctuations of simulated quanta. Columns **A** and **B** were obtained for matrices with 57 and 505 channels available, respectively, and with the same parameter sets (10,000 transmitter molecules released; $\alpha = 500$, $\beta = 10{,}000$). (Top row) Number of double-bound opened channels, expressed (A) in absolute value or (B) as percent of maximum in successive runs. (Bottom row) Superimposed waveforms of mean responses and σ, their standard deviations (left and right ordinates, respectively); $n = 12$. The coefficients of variation at the quantal summits are 3.8 and 1.7% in (A) and (B), respectively.

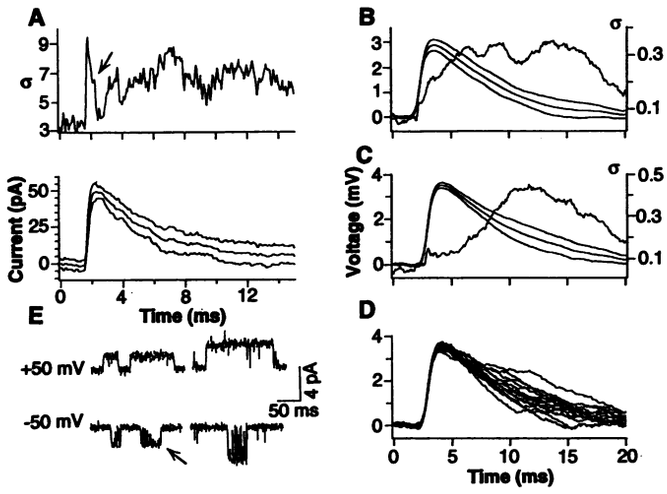

Fig. 3. Experimental validation of the model, showing increased variance throughout quantal events. Data obtained from the M cell soma of embryonic zebrafish (**A** and **E**) and of adult goldfish (**B** to **D**). (A) Whole-cell recording (at −50 mV) of spontaneous inhibitory postsynaptic currents in the presence of tetrodotoxin (TTX, 1 μM), with their standard deviation (above) and mean ± 1 SD (below), for responses with amplitudes from 45 to 55 pA (n = 20); arrow indicates the standard deviation at peak. (E) Examples of long-lasting single Cl^- channel currents activated by glycine (10 μm) and monitored at indicated potentials (outside-out configurations, symmetric Cl^-) with two elementary conductance states of 80 and 40 (arrow) pS, the latter being dominant in all patches. Thus, quanta in this preparation correspond to about 25 opened channels. (B and C) Similar analysis as in (A) with superimposed mean and standard deviation waveforms (n = 34) for intracellularly recorded miniature depolarizing inhibitory postsynaptic potentials (IPSPs) (2 μM TTX) falling in a large [2.4 to 3.5 mV (B)] and smaller [3.4 to 3.9 mV (C)] amplitude range. (D) Superimposed IPSPs used for (C) (n = 20). Note that even with a large number of channels in a quantum (500 to 1000) there are pronounced fluctuations in the waveform.

Figures 1 and 2 emphasize the difference between results of these simulations and those of models with analytical solutions of simultaneous differential equations. Although the latter produce smooth reproducible curves (*1*, *2*, *24*), Monte Carlo results are "noisy" and fluctuate in size and shape from one trial to the next, with variations in peak amplitude inconsistent with saturation. Figure 2 contrasts findings obtained with 57 (Fig. 2A) and 505 (Fig. 2B) channels per "cluster." The superimposed traces in Fig. 2A (top) exhibit significant fluctuations both at their peaks and during their decays, due to stochastic openings and closings of single channels. The mean response and standard deviation waveforms (Fig. 2A) demonstrate that even with few channels available less than 100% are opened, the CV is ~4% at peak, and there is an elevated variance during both the rising and falling phases. Similar results are predicted for the larger quantum (Fig. 2B, bottom). Figure 2B (top) further shows that although all binding sites are occupied (saturated) immediately after exocytosis, this process does not mean that all channels are opened at the same time.

When the standard deviation waveform (STDW) has been used to assess quanta in the central nervous system, it had been expected to parallel the time course of the mean with response shape stereotyped and variance due to differences in the amount of transmitter released or receptor number (*25*). In contrast, the simulations predict that stochastic channel behavior introduces variance, with the mean and STDW having different time courses. To test the validity of this conclusion, and more generally of the Monte Carlo model, we analyzed inhibitory quanta recorded from M cells of embryonic zebrafish and adult goldfish. Quanta involving few channels were collected with patch-clamp techniques from the intact zebrafish brain, in which the M cell can be visualized directly. In the experiment of Fig. 3A, their amplitude distribution had a mean of 50 pA. As predicted, the STDW has two peaks, one preceding that of the mean and one later during the decay phase. Because single glycine-activated Cl^- channels have a dominant conductance level of 40 pS (Fig. 3E) with a unitary current of 2 pA, the quantal currents corresponded to only ~25 opened channels (*26*). A similar discrepancy between mean and standard deviation time courses was obtained for larger quantal inhibitory postsynaptic potentials from the goldfish M cell (Fig. 3, B to D) (*10*). Because these responses were generated at several synapses in contrast to the simulations, we compared results obtained with events selected from wide (Fig. 3B) and narrow (Fig. 3, C and D) ranges within the unimodal distribution of somatic quanta (*10*). We expected that analysis of the latter would maximize detection of intrinsic variations. There was a marked increase in the standard deviation during the falling phase of the responses in both cases, with the CV less at the peak when we analyzed responses of almost exactly the same size (Fig. 3C). Superposition of those events illustrates the divergence of their decays (Fig. 3D).

The preceding findings confirmed the model's predictions and usefulness in assessing saturation and the relative contributions of different sources to quantal variability. As shown in Fig. 4A, typically 75 to 80% of the channels are opened at the peak of a quantum, with this value decreasing only slightly as q increases. The percentages of binding sites occupied either maximally or later, at the time of the peak (see Fig. 2B), exhibit the same trend. The overall conclusion is that binding reaches 100% within 100 μs after release. It is also less at the peak of the response, with an even

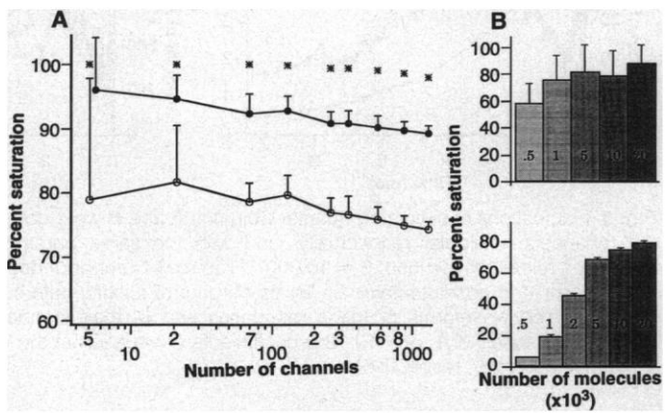

Fig. 4. Lack of saturation over a wide range of quantal size. (**A**) Plot of the percent saturation of the indicated variables (ordinate) versus the total number of channels included in a postsynaptic receptor matrix (abscissa). Each point (n = 20) is the mean + 1 SD. Although nearly 100% of the sites are occupied during the rising phase (see Fig. 2B), smaller and relatively constant fractions are bound and opened at the peak of the response, with a coefficient of variation that is largest for the small quanta. (Simulations with 10,000 molecules; α = 500, β = 5000.) (**B**) Effects of "vesicular contents" on response properties. Bar plots of mean q (% saturation, n = 10 to 20) + 1 SD, as a fraction of the number of molecules released, for aggregates with 5 (upper) and 900 (lower) channels. Note that response amplitudes are relatively insensitive to the amount of transmitter, except when the number of molecules and the number of available channels are approximately the same [α, β as in (A)]. Maximum sites bound, asterisk; sites bound at peak, filled circles; A_2R^* at peak, open circles.

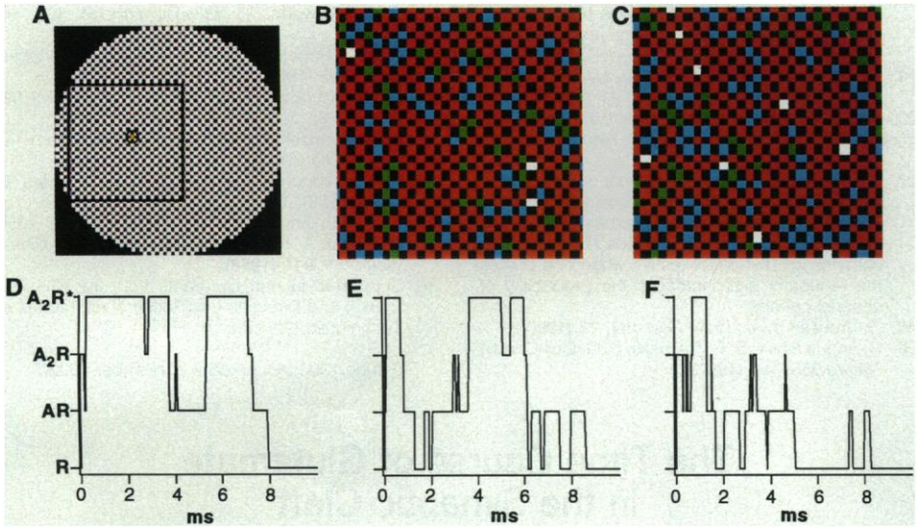

Fig. 5. Stochastic behavior of receptors during successive quantal responses. (**A**) En face view of a typical postsynaptic aggregate before release; cells devoid of receptors are black. The large square and the enclosed circle mark the region shown at higher magnifications to the right and the location of the single channel used for the state diagrams below, respectively. (**B** and **C**) Digital color images from two runs at the quantal peak (0.5 ms) with the following receptor numbers: A_2R^* (red), 1002 and 948; A_2R (green), 94 and 106; AR (blue), 204 and 230; and R (white), 13 and 29 (same conditions as in Fig. 1). (**D** to **F**) History of the identified channel from three separate simulations. These plots represent the closed states, with the channel only opened in the A_2R^* configuration. The model predicts repetitive openings of the channel and rebinding of transmitter. (α = 500, β = 5000.)

smaller and fluctuating fraction of the channels open at that time. Thus, neither true saturation nor invariance ever occurs. Furthermore, the inherent variability at a single site is greatest for the smallest quanta, CV ranging from 26% for five available channels per site to only ~3% for a matrix of 1300. One can appreciate this last observation by noting that while one channel is 20% of the total population when only five are involved, it represents less than 0.1% for the larger cluster.

Other factors also increase variability of quantal size. First, these events may be sensitive to differences in T, the amount of transmitter molecules released, although the effect is minimal for small quanta (Fig. 4B, top). A single value cannot be assigned to the additional CV introduced by this parameter because, in contrast to previous suggestions (*11*), the relation between quantal size and T is nonlinear. Figure 4B (bottom) shows that the quantum produced at a large receptor matrix is increased by about 7.5% when T is doubled from 5,000 to 10,000 (*27*). Second, active zones are not point sources and have diameters ≥0.1 μm (*16, 28*). Our computations indicate that off-center release introduces an additional CV of about 2 to 4% for the larger events (not shown). Thus, quanta generated at one site can be expected to have CVs, due to all sources considered, of at least 10 to 20%. Channel properties are most significant when quantal size is small, in the range of that estimated for several central synapses (*3, 10–12, 29*).

The model outputs graphically illustrate consequences of stochastic aspects of transmitter binding and channel gating. In Fig. 5, there were 1313 channels in the postsynaptic matrix. The color-coded images of the receptor states in one-fourth of that region during two simulated responses (0.5 ms after release) have quite different patterns. Similarly, when the history of one channel was extracted for three successive simulations (Fig. 5, D to F), it underwent a series of "unpredictable" state transitions, including multiple openings similar to those in the single-channel records. This "flicker," which could not be predicted with analytical solutions, provides another validation of the Monte Carlo simulations.

The intrinsic trial-to-trial variations in quantal responses are analogous to fluctuations seen in studies of many other ion channels and form the basis of the nonstationary fluctuation analysis developed by Sigworth (*30*). Briefly, there is a parabolic relation between the variance of an ionic current and its mean, with a maximum variance when P_o, the probability of a channel being open, = 0.5. Thus, for the same average number of opened channels on the rising and falling phases of a quantum, the standard deviation should be the same (Figs. 2 and 3). The observed decrease in variance between these two phases indicates that the maximal P_o exceeds 0.5. If the efficiency of channel opening were decreased (maximal $P_o < 0.5$), the CV would be greatest at the peak and the STDW might more closely approximate the average time course. This last condition could be achieved by reduction of the forward rate constants to simulate quantal events with longer rise times. However, those responses would have even larger variations in peak amplitude than described here.

In experiments on excitatory central synapses involving a small number of *N*-methyl-D-aspartate receptors, single-channel events were apparent and led to significant variations in the responses (*29, 31*), as suggested here. In fact, quanta at these and other synapses would only be invariant if $P_o = 1$, and to our knowledge this condition has not been observed. According to our simulations, it could only be met by an increase in β or a decrease in the back rate constants, thereby producing excessively long-lasting responses. Thus, reports of an STDW equal to zero at some central excitatory synapses (*6*) probably reflect inadequate separation of quantal responses from background noise rather than saturation.

At the neuromuscular junction there is a large excess of receptors (*32*), saturation does not occur (*33*), and q has pre- and postsynaptic determinants with variability primarily from differences in vesicle filling. However, as shown here, q at central synapses seems to be insensitive to vesicle filling. It follows that the postsynaptic membrane is the main determinant of q and its variability, even when there are restricted aggregates of receptor-channel complexes as with glycinergic (*34*) and, most likely, glutamatergic transmission. In any case, the fluctuations of q confirm that n and P retain their classical presynaptic significance. Under these conditions, changes in q, such as suggested for long-term potentiation in the hippocampus (*13, 14*), would be due to a postsynaptic modification (*35*). This conclusion would be required because the responses would not be significantly altered by an increase in the amount of transmitter released. Finally, quantal analysis requires accurate information about the size of a quantum and its variance at the junctions being investigated (*15*). This can best be accomplished in the central nervous system by measurement of responses evoked by one or a few presynaptic cells, because these properties are masked by the distribution of spontaneous q generated by the other inputs to a neuron.

REFERENCES AND NOTES

1. D. S. Faber, P. G. Funch, H. Korn, *Proc. Natl. Acad. Sci. U.S.A.* **82**, 3504 (1985).
2. C. Busch and B. Sakmann, *Cold Spring Harbor Symp. Quant. Biol.* **55**, 69 (1990).

3. F. A. Edwards, A. Konnerth, B. Sakmann, *J. Physiol. London* **430**, 213 (1990).
4. S. W. Kuffler and D. Yoshikami, *ibid.* **251**, 465 (1975).
5. F. Edwards, *Nature* **350**, 271 (1991).
6. F. R. Edwards, S. J. Redman, B. Walmsley, *J. Physiol. London* **259**, 689 (1976); J. J. B. Jack, S. J. Redman, K. Wong, *ibid.* **321**, 65 (1981).
7. H. Korn and D. S. Faber, *Trends Neurosci.* **14**, 439 (1991).
8. H. Korn, A. Mallet, A. Triller, D. S. Faber, *J. Neurophysiol.* **48**, 679 (1982).
9. H. Korn, Y. Burnod, D. S. Faber, *Proc. Natl. Acad. Sci. U.S.A.* **84**, 5981 (1987); H. Korn and D. S. Faber, *J. Neurophysiol.* **63**, 198 (1990).
10. N. Ropert, R. Miles, H. Korn, *J. Physiol. London* **428**, 287 (1990).
11. J. M. Bekkers, G. B. Richerson, C. F. Stevens, *Proc. Natl. Acad. Sci. U.S.A.* **87**, 5359 (1990).
12. J. M. Bekkers and C. F. Stevens, *Nature* **346**, 724 (1990); R. Malinow and R. W. Tsien, *ibid.*, p. 859; A. Margaroli and R. Tsien, *ibid.* **357**, 134 (1992).
13. T. D. Foster and B. L. McNaughton, *Hippocampus* 1, 79 (1991); D. M. Kullman and R. A. Nicoll, *Nature* **357**, 240 (1992).
14. T. Manabe, P. Renner, R. A. Nicoll, *Nature* **355**, 50 (1992).
15. H. Korn, C. Fassnacht, D. S. Faber, *ibid.* **350**, 282 (1991); D. S. Faber and H. Korn, *Biophys. J.* **60**, 1288 (1991).
16. A. Triller and H. Korn, *J. Neurophysiol.* **48**, 7081 (1982); our results are not changed by modification of total contact area, unless the receptor-free annulus is reduced drastically, producing a smaller q.
17. The average distance moved is obtained from the Einstein equation, with a Gaussian distribution function. See T. M. Bartol, Jr., B. R. Land, E. E. Salpeter, and M. M. Salpeter [*Biophys. J.* **59**, 1290 (1991)] for a detailed description of Monte Carlo simulations of miniature endplate currents, including methods for validating diffusion. The finer grid size used in that study increases computational time more than tenfold without altering q or kinetics.
18. The estimated number, n, of binding sites per glycine receptor is in the range of 2 to 3 [J. Diamond and S. Roper, *J. Physiol. London* **232**, 113 (1973); H. Akagi and R. Miledi, *Science* **242**, 270 (1988)]. In comparison with $n = 2$, responses simulated with $n = 3$ are 3 to 5% smaller at their peak, and their rise and half-decay times are 15 to 25% faster than those of the $n = 2$ responses. The possibility that the glycine receptor may have multiple open states, as in mouse spinal neurons [R. E. Twyman and R. L. MacDonald, *J. Physiol. London* **435**, 303 (1991)], was not incorporated into the model.
19. Transition probabilities are calculated from the matrix:

$$\begin{array}{c} \\ R \\ AR \\ A_2R \\ A_2R^* \end{array} \begin{array}{c} \begin{array}{cc} R\ (\text{free}) & AR\ (\text{single bound}) \end{array} \\ \begin{bmatrix} 1 - k_{+1}a\Delta t & k_{+1}a\Delta t \\ k_{-1}\Delta t & 1-(k_{-1} + k_{+2}a)\Delta t \\ 0 & k_{-2}\Delta t \\ 0 & 0 \end{bmatrix} \end{array}$$

$$\begin{array}{c} \\ R \\ AR \\ A_2R \\ A_2R^* \end{array} \begin{array}{c} \begin{array}{cc} A_2R\ (\text{double}) & A_2R^*\ (\text{open}) \end{array} \\ \begin{bmatrix} 0 & 0 \\ k_{+2}a\Delta t & 0 \\ 1 - (k_{-2} + \beta)\Delta t & \beta\Delta t \\ \alpha\Delta t & 1 - \alpha\Delta t \end{bmatrix} \end{array}$$

where the transitions are from the state in the first column to the state in the top row, a is the transmitter concentration in the "cell" above the receptor, and probabilities in each row sum to 1.
20. D. S. Faber and H. Korn, *J. Neurophysiol.* **60**, 1982 (1988).
21. ———, *Science* **208**, 612 (1980), *J. Neurophysiol.* **48**, 654 (1982).
22. A. B. Young and S. H. Snyder, *Proc. Natl. Acad Sci. U.S.A.* **70**, 2832 (1973).
23. Setting $k_{-2} = 10\ k_{-1}$ treats the two binding steps as nonequivalent, with the affinity higher for the first one. This relation applies to the nicotinic acetylcholine receptor [P. Blount and J. P. Merlie, *Neuron* **3**, 349 (1989)]; glycinergic responses simulated with equivalent binding give the same results presented here.
24. D. S. Faber and H. Korn, *Proc. Natl Acad. Sci. U.S.A.* **85**, 8708 (1988).
25. M. Solodkin *et al.*, *J Neurophysiol* **65**, 927 (1991)
26. P. Legendre and H. Korn, *Soc. Neurosci Abstr*, **18**, 1357 (1992).
27. Because the responses are not saturated, an increase in the background transmitter concentration in the synaptic cleft, for example, by lateral diffusion from adjacent synapses (*10*) could still enhance q. This effect results when one primes the receptors and increases the probability of channel opening.
28. G. Vrensen *et al*, *Brain Res* **184**, 23 (1980)
29. R. Angus Silver, S. F. Traynelis, S. G. Cull-Candy, *Nature* **355**, 163 (1992).
30. F. J Sigworth, *J Physiol London* **307**, 97 (1980).
31. H. P C Robinson, Y Sahara, N Kawai, *Biophys. J* **59**, 295 (1991)
32. H C. Fertuck and M M Salpeter, *J. Cell Biol* **69**, 144 (1976).
33. H. C Hartzell, S W Kuffler, D Yoshikami, *J Physiol. London* **251**, 427 (1975)
34. T Seitanidou, A Triller, H Korn, *J. Neurosci.* **8**, 4319 (1988)
35. G. Lynch and M Baudry, *Science* **224**, 1057 (1984), J. A. Kauer, R C Malenka, R A Nicoll, *Neuron* 1, 911 (1988).
36. Supported in part by grants from the NIH (NS 21848) and Direction des Recherches, Etudes et Techniques (92/058).

9 June 1992, accepted 8 September 1992

The Time Course of Glutamate in the Synaptic Cleft

John D. Clements,* Robin A. J. Lester,† Gang Tong, Craig E. Jahr, Gary L. Westbrook

The peak concentration and rate of clearance of neurotransmitter from the synaptic cleft are important determinants of synaptic function, yet the neurotransmitter concentration time course is unknown at synapses in the brain. The time course of free glutamate in the cleft was estimated by kinetic analysis of the displacement of a rapidly dissociating competitive antagonist from *N*-methyl-D-aspartate (NMDA) receptors during synaptic transmission. Glutamate peaked at 1.1 millimolar and decayed with a time constant of 1.2 milliseconds at cultured hippocampal synapses. This time course implies that transmitter saturates postsynaptic NMDA receptors. However, glutamate dissociates much more rapidly from α-amino-3-hydroxy-5-methyl-4-isoxazolepropionic acid (AMPA) receptors. Thus, the time course of free glutamate predicts that dissociation contributes to the decay of the AMPA receptor–mediated postsynaptic current.

The time course of neurotransmitter in the synaptic cleft has not been directly measured. At the frog neuromuscular junction, the time course of free acetylcholine (ACh) has been estimated from the shape of miniature end-plate currents (*1*) and is brief, principally due to rapid hydrolysis of ACh by acetylcholinesterase (*2*). Central glutamate-mediated synapses differ from the neuromuscular junction in that transmitter clearance depends on diffusion and reuptake rather than enzymatic breakdown (*3*). Central synapses also differ in their morphology (*4, 5*) and quantal characteristics of transmitter release (*6, 7*). The time course of free glutamate at hippocampal synapses must account for both fast and slow excitatory postsynaptic currents (EPSCs) mediated by co-localized AMPA and NMDA receptors (*8*). Although transmitter clearance is not the rate-limiting factor for the NMDA receptor–mediated EPSC (*9*), rapid desensitization of AMPA receptors (*10*) could mask the persistence of free transmitter. A detailed understanding of transmission at these synapses requires knowledge of the time course of glutamate in the cleft.

We estimated the concentration time course of free glutamate in the cleft by measuring the nonequilibrium reduction of NMDA receptor–mediated EPSCs produced by the rapidly dissociating antagonist D-aminoadipate (D-AA) (*11*). This antagonist is expected to reduce transmission by an amount proportional to its equilibrium occupancy of the postsynaptic receptors, less an amount due to glutamate displacement of D-AA on some receptors. The longer that transmitter is present, the more D-AA will be replaced by glutamate. This process provides a means to estimate the peak concentration and duration of transmitter at the postsynaptic membrane. To determine the transmitter time course by this method, several parameters must be known. These include the number of agonist and antagonist binding sites per recep-

J. D Clements and R A. J. Lester, Vollum Institute, Oregon Health Sciences University, Portland, OR 97201.
G Tong and C. E Jahr, Vollum Institute and Department of Cell Biology and Anatomy, Oregon Health Sciences University, Portland, OR 97201
G. L. Westbrook, Vollum Institute and Department of Neurology, Oregon Health Sciences University, Portland, OR 97201.

*To whom correspondence should be addressed
†Present address: Department of Molecular Physiology and Biophysics, Baylor College of Medicine, One Baylor Plaza, Houston, TX 77030